Exchange-correlation energy from Green's functions

Steven Crisostomo*
Department of Physics and Astronomy, University of California, Irvine, CA 92697, USA

E.K.U. Gross
Fritz Haber Center for Molecular Dynamics, Institute of Chemistry, The Hebrew University of Jerusalem, Jerusalem 91904, Israel

Kieron Burke
Department of Chemistry, University of California, Irvine, CA 92697, USA and Department of Physics and Astronomy, University of California, Irvine, CA 92697, USA

(Dated: March 3, 2024)

DFT calculations yield useful ground-state energies and densities, while Green's function techniques (such as GW) are mostly used to produce spectral functions. From the Galitskii-Migdal formula, we extract the exchange-correlation of DFT directly from a Green's function. This spectral representation provides an alternative to the fluctuation-dissipation theorem of DFT, identifying distinct single-particle and many-particle contributions. Results are illustrated on the uniform electron gas and the two-site Hubbard model.

Ground-state density functional theory [1, 2] (DFT) is used to great effect in modern molecular and materials calculations, limited only by the approximation for the exchange-correlation (XC) energy [3]. But there is also interest in the response properties of a system, such as its spectral function and associated gap [4]. While range-separated hybrids can yield moderately accurate gaps within the generalized KS scheme [5–7], the standard method for gaps remains GW calculations [8, 9]. For strongly-correlated materials, dynamical mean field theory has become a very useful tool [10, 11].

Such Green's function (GF) methods come from traditional many-body theory. KS-DFT does not, and it is difficult to relate the two. This leads to issues whenever, as is common practice, a DFT calculation is used to find some set of KS orbitals, which form the starting point of GF calculations [12]. The choice of initial orbitals can be important [13–15], while a self-consistent GF can eliminate this dependence [16–19]. The XC energy of DFT is traditionally analyzed in terms of static quantities extractable from the ground-state wave-function, such as the XC hole, the dearth of conditional electronic density around an electron [20–22]. If a frequency decomposition is performed, it is in terms of the density-density response function [23].

We provide a bridge between these two distinct approaches by extracting the contribution to the XC energy directly from an interacting GF. Our GXC formula can be used to (a) extract approximate XC energies from approximate GF, (b) provide a novel decomposition of XC energies into single-particle and many-particle contributions, (c) provide models for existing DFT approximations in terms of GF, (d) relate the quality of spectral functions to their performance for XC energies. We illustrate our results on the uniform electron gas and the two-site Hubbard model.

* crisosts@uci.edu

Consider Hamiltonians of the form (in Hartree atomic units)

$$\hat{H} = \sum_{j}^{N} \hat{h}(\mathbf{r}_i) + \sum_{i>j}^{N} \hat{V}_{\rm ee}(|\mathbf{r}_i - \mathbf{r}_j|), \tag{1}$$

where $\hat{h}(\mathbf{r}) = \hat{t}(\mathbf{r}) + v(\hat{\mathbf{r}})$ is the single-particle Hamiltonian, with kinetic energy operator $\hat{t} = -\nabla^2/2$, multiplicative spin-independent external potential $v(\hat{\mathbf{r}})$, and $\hat{V}_{\rm ee}(u) = 1/u$ is the Coulomb repulsion between pairs of electrons. We work within the Born-Oppenheimer approximation in the non-relativistic limit, with no external magnetic fields. We use $\mathbf{x} = (\mathbf{r}, \sigma)$ as a space-spin coordinate, and $n(\mathbf{x})$ is the ground-state spin density.

Within spin-DFT, the corresponding KS system consists of fictitious non-interacting electrons with the same ground-state density as the interacting system. The exact ground-state energy is then

$$E = T_{\rm S} + V + E_{\rm HXC}, \tag{2}$$

where $T_{\rm S}$ is the kinetic energy of non-interacting electrons, V is the external potential energy, and $E_{\rm HXC}$ is the sum of the Hartree (electrostatic) and XC energies. The KS potential is

$$v_{\rm S}(\mathbf{x}) = v(\mathbf{r}) + v_{\rm HXC}(\mathbf{x}), \tag{3}$$

where $v_{\rm HXC}(\mathbf{x}) = \delta E_{\rm HXC}[n]/\delta n(\mathbf{x})$. The KS equations are solved self-consistently, yielding the exact density and energy given the exact XC [24].

The time-ordered Green's function is

$$G(\mathbf{x}t, \mathbf{x}'t') = -\big\langle \mathcal{T}\big[\hat{\psi}(\mathbf{x}t)\hat{\psi}^\dagger(\mathbf{x}'t')\big]\big\rangle, \tag{4}$$

where $\mathcal{T}$ is the time-ordering operator and $\langle\cdot\rangle$ denotes the expectation value over the N-electron ground-state $|\Psi_0\rangle$. The fermionic operators, $\hat{\psi}^\dagger(\mathbf{x})$ and $\hat{\psi}(\mathbf{x})$, create and

destroy a particle of spin σ at $\mathbf{r}$ and are time-evolved in the Heisenberg picture according to $\hat{H}$. For time-independent $\hat{H}$, we denote the Fourier transform $G(\mathbf{x},\mathbf{x}',\omega)$. We define

$$\mathrm{Tr}\{F\} = -i\int \frac{d\omega}{2\pi}\,\mathrm{tr}\{F\}, \tag{5}$$

where a convergence factor $\exp(i\omega\delta)$ with $\delta \to 0^+$ is implied, to respect time-ordering ($t' \to t^+$). Here tr denotes

$$\mathrm{tr}\{F\} = \int d^3r \sum_{\sigma=\sigma'} \lim_{\mathbf{r}'\to\mathbf{r}} F(\mathbf{x},\mathbf{x}',\omega). \tag{6}$$

The Galitskii-Migdal (GM) formula [25] yields the total interacting ground-state energy from the GF

$$E = \frac{1}{2}\,\mathrm{Tr}\{(\omega + \hat{h}(\mathbf{r}))G\}. \tag{7}$$

To isolate XC, apply GM to the KS system,

$$E_\mathrm{S} = \frac{1}{2}\,\mathrm{Tr}\{(\omega + \hat{h}_\mathrm{S}(\mathbf{x}))G_\mathrm{S}\}. \tag{8}$$

Subtraction yields GXC, the GF XC contribution

$$G_\mathrm{XC} = E_\mathrm{XC} - \frac{\langle v_\mathrm{XC}\rangle}{2} = \frac{1}{2}\,\mathrm{Tr}\left\{\left(\omega + \hat{t}(\mathbf{r})\right)\Delta G\right\}, \tag{9}$$

where $\Delta G = G - G_\mathrm{S}$. More explicitly

$$G_\mathrm{XC} = -\frac{i}{2}\int d^3r \lim_{u\to 0}\int \frac{d\omega}{2\pi}\left(\omega - \frac{\nabla_\mathbf{u}^2}{2}\right)\Delta G(\mathbf{r},\mathbf{r}+\mathbf{u},\omega), \tag{10}$$

where $\Delta G(\mathbf{r},\mathbf{r}+\mathbf{u},\omega)$ is an analog of the XC hole. Like the XC hole, obeying sum rules. Without the ω term, Eq. (10) yields T_C. Moreover

$$-i\int \frac{d\omega}{2\pi}\,\Delta G(\mathbf{r},\mathbf{r},\omega) = 0, \tag{11}$$

because both Green's functions have the same density. An early version appeared [26] even before the adiabatic connection formula of DFT was precisely defined [23, 27].

First, Eq. (9) provides a method for extracting an XC contribution directly from any GF. At the end of any GF calculation, the density of G can be extracted, a KS inversion [28–32] performed and the corresponding G_S constructed. But G_XC is not E_XC. Given an explicit approximation for E_XC, it is easy to construct G_XC, but not vice versa. Thus, for a non-self-consistent GW calculation (the vast majority), a measure of inconsistency would be G_XC of the original DFT calculation versus that of Eq. (9). A self-consistent calculation would presumably satisfy Eq. (9) on its final iteration. An important feature of G_XC is that it can be used to construct the total energy from the sum of KS orbital energies E_S:

$$E = E_\mathrm{S} + \left(G_\mathrm{XC} - \frac{\langle v_\mathrm{HXC}\rangle}{2}\right). \tag{12}$$

Thus G_XC is related to a double-counting correction.

Now we use Eq. (9) to create a novel decomposition of XC energies in DFT. Define the energy difference

$$\omega_J = E_0(N) - E_J(N-1), \tag{13}$$

where $E_J(M)$ is the energy of the Jth interacting eigenstate of the M-electron system; $J=0$ denotes the ground-state. Then the Lehmann representation is

$$G(\mathbf{x},\mathbf{x}',\omega) = \sum_J \frac{\rho_J(\mathbf{x},\mathbf{x}')}{\omega - \omega_J - i\delta} + \sum_{J'} \frac{\bar{\rho}_{J'}(\mathbf{x},\mathbf{x}')}{\omega - \bar{\omega}_{J'} + i\delta}, \tag{14}$$

where the spectral weights are

$$\rho_J(\mathbf{x},\mathbf{x}') = \langle\Psi_0|\hat{\psi}^\dagger(\mathbf{x}')|J\rangle\langle J|\hat{\psi}(\mathbf{x})|\Psi_0\rangle. \tag{15}$$

Here $\{|J\rangle\}$ are the interacting eigenstates of the N-1-electron system, while $\bar{\rho}_{J'}(\mathbf{x},\mathbf{x}')$ is defined analogously, with fermionic operators in Eq. (15) swapped, and $\{|J'\rangle\}$ enumerating eigenstates of the $N+1$-electron system. The sum over J of $\rho_J(\mathbf{x},\mathbf{x}')$ is simply the first-order density matrix. Likewise, we write

$$G_\mathrm{S}(\mathbf{x},\mathbf{x}',\omega) = \sum_j \frac{\rho_{s,j}(\mathbf{x},\mathbf{x}')}{\omega - \epsilon_j - i\delta} + \sum_{j'} \frac{\bar{\rho}_{s,j'}(\mathbf{x},\mathbf{x}')}{\omega - \bar{\epsilon}_{j'} + i\delta}, \tag{16}$$

where j runs over KS orbitals and we consider only the occupied orbitals. Inserting into Eq. (9) yields

$$G_\mathrm{XC} = \frac{1}{2}\sum_J (T_J + \omega_J f_J) - \sum_j (T_{s,j} + \epsilon_j f_{s,j}), \tag{17}$$

where T_J is the kinetic contribution from state J and $f_J = \mathrm{tr}\{\rho_J\}$ are the 'occupations' of each state, with analogous contributions from the KS system. They satisfy the sum rule that each, when summed over all occupied states, yields N.

To make further progress, we relate the two sums in Eq. (17) via the adiabatic connection of DFT. Multiply V_ee in Eq. (1) by λ while choosing a λ-dependent one-body potential to keep the density fixed [33]. As $\lambda \to 0$, a subset of J approaches the KS orbitals and eigenvalues. We call these single-particle contributions (SP), the rest many-particle (MP). We denote sums over such excitations by K. This is analogous to how we define single-particle excitations in TDDFT [34]. Thus

$$G_\mathrm{XC} = G_\mathrm{XC}^\mathrm{SP} + G_\mathrm{XC}^\mathrm{MP}, \tag{18}$$

where the SP contribution is

$$G_\mathrm{XC}^\mathrm{SP} = \frac{1}{2}\sum_j (T_{\mathrm{C},j} + \omega_j f_j - \epsilon_j f_{\mathrm{s},j}), \tag{19}$$

and $T_{\mathrm{C},j} = T_j - T_{\mathrm{s},j} = \mathrm{tr}\{t(\mathbf{r})(\rho_j - \rho_{\mathrm{s},j})\}$ is the contribution to the correlation kinetic energy from each SP state. The many-particle contributions are purely correlation

$$G_\mathrm{C}^\mathrm{MP} = \frac{1}{2}\sum_K (T_K + \omega_K f_K). \tag{20}$$

In the SP contribution, the highest occupied KS level is special, as KS-DFT guarantees that the HOMO KS eigenvalue is exactly minus the ionization potential, i.e., $\omega_0 = -I = \epsilon_0$. Labelling it as zero, we write

$$G^{\rm SP}_{{\rm XC},0} = \frac{1}{2}(T_{{\rm C},0} - I(f_0 - f_{{\rm s},0})). \tag{21}$$

The correlation kinetic energy, $T_{\rm C}$, is just the sum of its SP and MP contributions. We can analogously isolate contributions to the potential correlation energy. Their sum yields the correlation energy, so

$$E_{\rm XC} = E^{\rm SP}_{\rm XC} + E^{\rm MP}_{\rm C}, \tag{22}$$

i.e. individual peaks in the spectral function yield individual contributions to the $E_{\rm XC}$ energy. The exchange contribution is found by using the exchange self-energy (see SM), yielding

$$G_{\rm X} = \sum_j {\rm tr}\{(\Sigma_{\rm X}[G_{\rm S}] - v_{\rm X})\rho_{{\rm s},j}\} = G^{\rm SP}_{\rm X}. \tag{23}$$

For a two-electron singlet $G_{\rm X}$ vanishes.

Likewise, the ground-state density matrix is

$$\rho(\mathbf{x},\mathbf{x}') = \int_{-\infty}^{0} d\omega\, A(\mathbf{x},\mathbf{x}',\omega), \tag{24}$$

where the spectral function is

$$A(\mathbf{x},\mathbf{x}',\omega) = -\frac{1}{\pi}{\rm Im}\{G(\mathbf{x},\mathbf{x}',\omega)\}\,{\rm sgn}(\omega). \tag{25}$$

Thus ρ (and its diagonal, the ground-state density) also can be uniquely decomposed.

An alternative decomposition uses $\omega_j = -I - \Delta E_j$, where $\Delta E_j = E_j(N-1) - E_0(N-1) \geq 0$ are the transition frequencies. Then

$$G_{\rm XC} = G^{\rm SPI}_{\rm XC} + G^{\rm MPI}_{\rm C}, \tag{26}$$

with different SP and MP contributions

$$G^{\rm SPI}_{\rm XC} = \frac{1}{2}\sum_j \left[T_{c,j} - (\Delta E_j f_j - \Delta E_{s,j} f_{s,j})\right], \tag{27}$$

$$G^{\rm MPI}_{\rm C} = \frac{1}{2}\sum_K \left[T_K - \Delta E_K f_K\right]. \tag{28}$$

In particular, $G^{\rm SPI}_{xc,0} = T_{c,0}/2$. Each decomposition is useful in different circumstances.

The asymmetric two-site Hubbard model [35, 36] is particularly well-suited as an illustration, because of its extremely truncated Hilbert space. We have two femions in the Hamiltonian,

$$-t\sum_\sigma \left(\hat{c}^\dagger_{1\sigma}\hat{c}_{2\sigma} + {\rm h.c.}\right) + U\sum_{j=1}^{2}\hat{n}_{j\uparrow}\hat{n}_{j\downarrow} + \sum_{j=1}^{2} v_j\hat{n}_j, \tag{29}$$

where t is the hopping term, U the on-site interaction strength, $\hat{n}_j$ the site-occupation operator, and $\hat{c}^\dagger_{j\sigma}$, $\hat{c}_{j\sigma}$ are the fermionic operators associated to each site. Only the potential difference $\Delta v = v_2 - v_1$ matters. The ground-state is a singlet, and its density is characterized by one number, $\Delta n = n_2 - n_1$. KS-DFT applies [35] and the KS system is simply the tight-binding dimer.

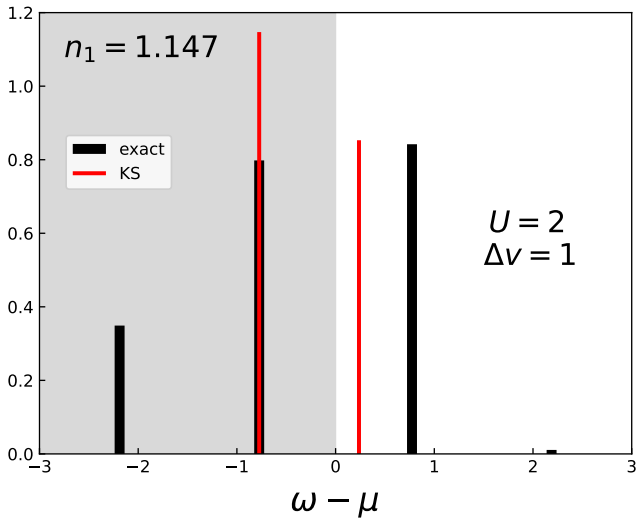

FIG. 1: Hubbard dimer local spectral functions $A_{11}(\omega)$ (black) and $A_{{\rm s},11}(\omega)$ (red). Here $\mu = U/2$ and $t = 1/2$. The spectral weight below 0 sums to $n_1 = 1.147$, and above to n_2.

Figure 1 shows a typical spectral function [35] with bars whose height is the pole weight. G has 4 poles, two for removal and two for gain, but $G_{\rm S}$ has only one of each. The difference between the two central peaks is the gap, with the KS gap famously being smaller than the true gap [37, 38]. Only the removal peaks contribute to XC. The larger exact peak is the only single-particle contribution, and the smaller is a many-particle. By Eq. (24), they sum to n_1, and the KS peak must be higher. The many-particle contributes negatively to $G_{\rm XC}$ while SP contributes positively, a delicate balance.

U	$E_{\rm XC}$	$E_{\rm C}$	$G_{\rm XC}$	$G^{\rm SP}_{\rm XC}$	$G^{\rm MP}_{\rm XC}$	$G^{\rm SPI}_{\rm XC}$	$G^{\rm MPI}_{\rm XC}$
0.5	-0.339	-0.01062	-0.013	0.011	-0.024	0.00338	-0.0164
1	-0.643	-0.0676	-0.0524	0.0516	-0.104	0.0189	-0.0713
2	-1.39	-0.3666	-0.139	0.224	-0.363	0.0847	-0.224
4	-3.23	-1.224	-0.194	0.689	-0.883	0.188	-0.381
10	-9.1	-4.098	-0.206	2.16	-2.36	0.27	-0.476
20	-19.	-9.05	-0.207	4.64	-4.85	0.297	-0.504

TABLE I: XC of dimer with $t = 1/2$ and $\Delta v = 1$.

The first use of our formula is to identify how much each peak contributes to XC. Table I shows values of various quantities for a range of U. $G_{\rm XC}$ is comparable to $E_{\rm C}$ for

weak correlation (as $G_{\rm x} = 0$ for $N = 2$), but significantly smaller for strong correlation, with cancellation between SP and MP contributions. The alternative decomposition yields terms of much smaller magnitude, requiring a less delicate balance, especially for large U.

Z	$E_{\rm XC}$	$\langle v_{\rm XC}\rangle/2$	$E_{\rm C}$	$T_{\rm C}$	$G_{\rm XC}$
1	-0.4229	-0.3562	-0.04199	0.02788	-0.06667
2	-1.067	-1.01	-0.04211	0.03664	-0.05691
3	-1.695	-1.638	-0.04352	0.03983	-0.05627
4	-2.321	-2.265	-0.04427	0.04148	-0.05604
6	-3.572	-3.516	-0.04506	0.04318	-0.05584
10	-6.073	-6.017	-0.04569	0.04456	-0.0557
20	-12.32	-12.27	-0.04618	0.0456	-0.0556

TABLE II: XC for the two-electron ions [39].

For realistic DFT calculations, as the local density approximation yields $E_{\rm x}^{\rm LDA}[n] = -A_{\rm x}\int n^{4/3}(\mathbf{r})$, typically $G_{\rm XC} \approx E_{\rm XC}/3$, especially for large N. For $N = 2$, we cannot assume Hubbard results are typical, but (essentially) exact DFT calculations have been performed for two-electron ions (Table II) and Hooke's atom (quadratic confining potential in the SM), where $G_{\rm C}$ is comparable to $E_{\rm C}$ in magnitude.

The LDA can be understood as a local approximation to the XC hole [40, 41], as the system- and spherically averaged LDA XC hole reflects the accuracy of LDA [42]. The real-space construction of the GGA from the gradient expansion for the hole underlies both the PW91 and PBE XC approximations [21, 43]. XC holes are also behind some of the most popular functionals in chemistry [20, 22, 43]. Now we derive $G_{\rm XC}^{\rm LDA}$ from an ansatz for the Green's function. Define $\Delta G^{\rm UEG}(n,u,\omega)$ as the difference between exact and KS Green's functions of a uniform gas of density n, separation $u = |\mathbf{r}-\mathbf{r}'|$, and frequency ω. Approximating ΔG with $\Delta G^{\rm UEG}(n(\mathbf{r}),|\mathbf{r}-\mathbf{r}'|,\omega)$ in Eq. (9) directly yields

$$G_{\rm XC}^{\rm LDA} = \int d^3r\, g_{\rm XC}^{\rm UEG}(n(\mathbf{r})), \tag{30}$$

where $g_{\rm XC}^{\rm UEG}(n) = (2 - d/dn)e_{\rm XC}^{\rm UEG}(n)/2$ is the $G_{\rm XC}$ energy density, $\mathrm{Tr}\{(\omega + \hat{t}(u))\Delta G^{\rm UEG}\}/V$, and V is the volume. System-averaged and frequency-integrated quantities should agree to the extent that LDA yields reasonably accurate energies, but are there major cancellations of errors inside the frequency integral? And do approximate GF calculations improve this frequency dependence? These are the sorts of questions that can be explored with our formula.

Our final point concerns the approximate GF calculations that our formula is designed to analyze, illustrated for GW calculations on the Hubbard dimer. We use the Hartree-Fock GF to generate the initial GW self-energy and iterate until the energy convergences. Each iteration generates extra poles, but we retain only a few (see SM). If the self-energy has (correctly) only two poles, the next G^{GW} generally has six, instead of the correct four. But if we reduce the 6 poles of G to the correct 4, the self-energy has 4. We chose the former scheme for calculations here. To aid convergence, for cases with moderate to strong correlation we generated the nth GF according to: $G^{(n)} = \gamma G^{(n-1)} + (1-\gamma)G^{(n-2)}$, with $\gamma = 0.67$. Our one-shot results are identical to Ref [44] when $\Delta v = 0$.

Both the six-pole and four-pole G^{GW} yield the same density and $v_{\rm XC}$, but they differ considerably. Both satisfy the Sham-Schlüter equation at each iteration [38],

$$-i\int \frac{d\omega}{2\pi}\left[G_{\rm S}\Sigma G\right]_{ii} = -i\int \frac{d\omega}{2\pi}\left[G_{\rm S}v_{\rm HXC}G\right]_{ii}, \tag{31}$$

but have different kinetic and XC energies. For the dimer

$$G_{\rm XC} = \int_{-\infty}^{0} d\omega\left[\omega(\Delta A_{11}(\omega)+\Delta A_{22}(\omega)) - 2t\Delta A_{12}(\omega)\right], \tag{32}$$

where we have summed over spins and ΔA_{ij} is the difference in retarded spectral functions. Due to Eq. (11), the frequency integral of $\Delta A_{11}(\omega)+\Delta A_{22}(\omega)$ up to the chemical potentials yields 0. Fig. 2 shows ΔA_{11}, which comprises a majority of $G_{\rm XC}$, as ΔA_{22} gives a negligible contribution.

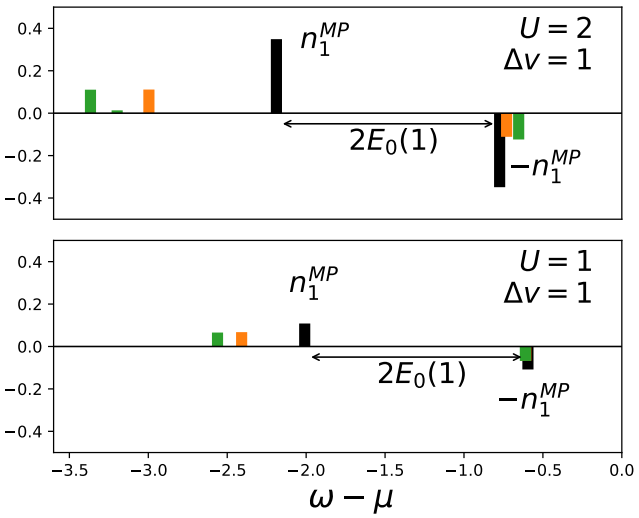

FIG. 2: Spectral function differences $\Delta A_{11}(\omega)$ with $\mu = U/2$ and $t = 1/2$. Exact (black), one-shot (orange), and self-consistent GW (green). The separation of the SP and MP poles is twice the energy of the one-particle groundstate, but GW introduces an erroneous interaction dependence.

From Fig. 2, the SP pole positions and heights for one-shot GW are more accurate than the self-consistent GW. Table III also shows a poorer approximation to $E_{\rm C}$, worsening with increasing U. However, full self-consistency produces better total energies for weak correlation, while in the strongly-correlated case, neither flavor of GW produces accurate energies (see SM).

	Exact			one-shot			self-consistent		
U	$G_{\rm XC}$	$G_{\rm XC}^{\rm SPI}$	$G_{\rm XC}^{\rm MPI}$	$G_{\rm XC}$	$G_{\rm XC}^{\rm SPI}$	$G_{\rm XC}^{\rm MPI}$	$G_{\rm XC}$	$G_{\rm XC}^{\rm SPI}$	$G_{\rm XC}^{\rm MPI}$
0.25	-3.05	0.67	-3.72	-4.88	1.12	-6.	-4.95	1.15	-6.1
0.5	-13.	3.38	-16.4	-15.9	4.4	-20.3	-16.9	4.69	-21.6
1	-52.4	18.9	-71.3	-41.9	14.4	-56.3	-54.8	16.2	-71.
2	-139.	84.7	-224.	-98.1	33.8	-132.	-186.	42.	-228.
4	-194.	188.	-381.	-232.	57.5	-289.	-583.	88.	-671.

	Exact			one-shot			self-consistent		
U	$E_{\rm C}$	$E_{\rm C}^{\rm SPI}$	$E_{\rm C}^{\rm MPI}$	$E_{\rm C}$	$E_{\rm C}^{\rm SPI}$	$E_{\rm C}^{\rm MPI}$	$E_{\rm C}$	$E_{\rm C}^{\rm SPI}$	$E_{\rm C}^{\rm MPI}$
0.25	-1.95	1.76	-3.71	-3.09	2.88	-5.97	-3.83	2.25	-6.08
0.5	-10.6	5.62	-16.2	-13.8	6.29	-20.1	-19.3	2.18	-21.5
1	-67.6	1.43	-69.	-68.1	-13.3	-54.9	-87.9	-16.5	-71.4
2	-367.	-142.	-225.	-288.	-153.	-135.	-292.	-56.3	-236.
4	-1220.	-627.	-597.	-798.	-463.	-335.	-761.	-60.	-701.

TABLE III: Decompositions for the asymmetric dimer with $t = 1/2$ and $\Delta v = 1$, in milliHartrees.

Practical GF calculations are performed on solids and molecules, with a variety of approximations, such as GW and dynamical mean field theory [45–49]. Once a KS inversion can be performed [30–32] on the density of the approximate GF, a value for $G_{\rm XC}$ can be extracted which can be compared with a DFT counterpart, especially when standard XC functionals are known to fail. However, molecules have both bound and continuum states, while all states are in continuua in solids, complicating the identification of SP and MP contributions. For GW, there are many different recipes yielding distinct spectral features [14, 16, 50, 51], but one must always use the KS GF of the density of the approximate GF, as the XC contributions depend on delicate cancellations, as illustrated here. Recently Ref. [52] shows that exact XC energies can be produced via approximate self-energies. Our work is complementary, with our focus primarily being representations of XC energies via approximate GF. Our systematic determination of sources of XC errors should aid in designing future alternative approximate density functionals or GF methods.

We thank Lucia Reining, Abdallah El-Sahili, and Vojtěch Vlček for valuable discussions. S.C. and K.B. were supported by NSF Award No. CHE-2154371. E.K.U.G acknowledges support form the European Research Council. This project has received funding from the European Research Council (ERC) under the European Unions Horizon 2020 research and innovation programme (Grant Agreement No. ERC-2017-AdG-788890).

[1] P. Hohenberg and W. Kohn, Inhomogeneous electron gas, Phys. Rev. **136**, B864 (1964).
[2] W. Kohn and L. J. Sham, Self-consistent equations including exchange and correlation effects, Phys. Rev. **140**, A1133 (1965).
[3] W. Kohn, Nobel Lecture: Electronic structure of matter—wave functions and density functionals, Rev. Mod. Phys. **71**, 1253 (1999).
[4] B. Lenz, C. Martins, and S. Biermann, Spectral functions of sr2iro4: theory versus experiment, Journal of Physics: Condensed Matter **31**, 293001 (2019).
[5] A. Seidl, A. Görling, P. Vogl, J. A. Majewski, and M. Levy, Generalized Kohn-Sham schemes and the band-gap problem, Phys. Rev. B **53**, 3764 (1996).
[6] J. P. Perdew, W. Yang, K. Burke, Z. Yang, E. K. U. Gross, M. Scheffler, G. E. Scuseria, T. M. Henderson, I. Y. Zhang, A. Ruzsinszky, H. Peng, J. Sun, E. Trushin, and A. Görling, Understanding band gaps of solids in generalized Kohn-Sham theory, Proceedings of the National Academy of Sciences **114**, 2801 (2017), https://www.pnas.org/doi/pdf/10.1073/pnas.1621352114.
[7] R. Garrick, A. Natan, T. Gould, and L. Kronik, Exact generalized kohn-sham theory for hybrid functionals, Phys. Rev. X **10**, 021040 (2020).
[8] L. Hedin, New Method for Calculating the One-Particle Green's Function with Application to the Electron-Gas Problem, Phys. Rev. **139**, A796 (1965).
[9] D. Golze, M. Dvorak, and P. Rinke, The GW Compendium: A Practical Guide to Theoretical Photoemission Spectroscopy, Frontiers in Chemistry **7**, 10.3389/fchem.2019.00377 (2019).
[10] A. Georges, G. Kotliar, W. Krauth, and M. J. Rozenberg, Dynamical mean-field theory of strongly correlated fermion systems and the limit of infinite dimensions, Rev. Mod. Phys. **68**, 13 (1996).
[11] E. Pavarini, S. Biermann, A. Poteryaev, A. I. Lichtenstein, A. Georges, and O. K. Andersen, Mott transition and suppression of orbital fluctuations in orthorhombic $3d^1$ perovskites, Phys. Rev. Lett. **92**, 176403 (2004).
[12] M. J. van Setten, F. Caruso, S. Sharifzadeh, X. Ren, M. Scheffler, F. Liu, J. Lischner, L. Lin, J. R. Deslippe, S. G. Louie, C. Yang, F. Weigend, J. B. Neaton, F. Evers, and P. Rinke, Gw100: Benchmarking g0w0 for molecular systems, Journal of Chemical Theory and Computation **11**, 5665 (2015), pMID: 26642984, https://doi.org/10.1021/acs.jctc.5b00453.
[13] F. Bruneval and M. A. L. Marques, Benchmarking the starting points of the gw approximation for molecules, Journal of Chemical Theory and Computation **9**, 324 (2013), pMID: 26589035, https://doi.org/10.1021/ct300835h.
[14] L. Reining, The gw approximation: content, successes and limitations, WIREs Computational Molecular Science **8**, e1344 (2018), https://wires.onlinelibrary.wiley.com/doi/pdf/10.1002/wcms.1344.
[15] S. E. Gant, J. B. Haber, M. R. Filip, F. Sagredo, D. Wing, G. Ohad, L. Kronik, and J. B. Neaton, Optimally tuned starting point for single-shot gw calculations of solids, Phys. Rev. Mater. **6**, 053802 (2022).
[16] M. van Schilfgaarde, T. Kotani, and S. Faleev, Quasiparticle self-consistent gw theory, Phys. Rev. Lett. **96**, 226402 (2006).

[17] F. Bruneval and M. Gatti, Quasiparticle self-consistent gw method for the spectral properties of complex materials, in *First Principles Approaches to Spectroscopic Properties of Complex Materials*, edited by C. Di Valentin, S. Botti, and M. Cococcioni (Springer Berlin Heidelberg, Berlin, Heidelberg, 2014) pp. 99–135.

[18] A. Förster and L. Visscher, Low-order scaling quasiparticle self-consistent gw for molecules, Frontiers in Chemistry **9**, 10.3389/fchem.2021.736591 (2021).

[19] C.-N. Yeh, S. Iskakov, D. Zgid, and E. Gull, Fully self-consistent finite-temperature gw in gaussian bloch orbitals for solids, Phys. Rev. B **106**, 235104 (2022).

[20] A. D. Becke, Correlation energy of an inhomogeneous electron gas: A coordinate-space model, The Journal of Chemical Physics **88**, 1053 (1988), https://pubs.aip.org/aip/jcp/article-pdf/88/2/1053/11192435/1053_1_online.pdf.

[21] J. P. Perdew, K. Burke, and M. Ernzerhof, Generalized gradient approximation made simple, Phys. Rev. Lett. **77**, 3865 (1996).

[22] C. Adamo and V. Barone, Toward reliable density functional methods without adjustable parameters: The PBE0 model, The Journal of Chemical Physics **110**, 6158 (1999), https://pubs.aip.org/aip/jcp/article-pdf/110/13/6158/10797469/6158_1_online.pdf.

[23] J. Harris and R. O. Jones, The surface energy of a bounded electron gas, Journal of Physics F: Metal Physics **4**, 1170 (1974).

[24] E. M. Stoudenmire, L. O. Wagner, S. R. White, and K. Burke, One-dimensional continuum electronic structure with the density-matrix renormalization group and its implications for density-functional theory, Phys. Rev. Lett. **109**, 056402 (2012).

[25] V. M. Galitskii and A. B. Migdal, Application of quantum field theory methods to the many body problem, Sov. Phys. JETP **7**, 18 (1958).

[26] L. J. Sham, Exchange and correlation in density-functional theory, Phys. Rev. B **32**, 3876 (1985).

[27] D. Langreth and J. Perdew, The exchange-correlation energy of a metallic surface, Solid State Communications **17**, 1425 (1975).

[28] S. Nam, S. Song, E. Sim, and K. Burke, Measuring density-driven errors using kohn–sham inversion, Journal of Chemical Theory and Computation **16**, 5014 (2020), pMID: 32667787.

[29] S. Nam, R. J. McCarty, H. Park, and E. Sim, Ks-pies: Kohn–sham inversion toolkit, The Journal of Chemical Physics **154**, 124122 (2021).

[30] Y. Shi and A. Wasserman, Inverse kohn–sham density functional theory: Progress and challenges, The Journal of Physical Chemistry Letters **12**, 5308 (2021), pMID: 34061541, https://doi.org/10.1021/acs.jpclett.1c00752.

[31] Y. Shi, V. H. Chávez, and A. Wasserman, n2v: A density-to-potential inversion suite. a sandbox for creating, testing, and benchmarking density functional theory inversion methods, WIREs Computational Molecular Science **12**, e1617 (2022), https://wires.onlinelibrary.wiley.com/doi/pdf/10.1002/wcms.1617.

[32] A. Aouina, M. Gatti, S. Chen, S. Zhang, and L. Reining, Accurate kohn-sham auxiliary system from the ground-state density of solids, Phys. Rev. B **107**, 195123 (2023).

[33] A. Savin, F. Colonna, and R. Pollet, Adiabatic connection approach to density functional theory of electronic systems, International Journal of Quantum Chemistry **93**, 166 (2003), https://onlinelibrary.wiley.com/doi/pdf/10.1002/qua.10551.

[34] N. T. Maitra, Double and charge-transfer excitations in time-dependent density functional theory, Annual Review of Physical Chemistry **73**, 117 (2022), pMID: 34910562, https://doi.org/10.1146/annurev-physchem-082720-124933.

[35] D. J. Carrascal, J. Ferrer, J. C. Smith, and K. Burke, The hubbard dimer: a density functional case study of a many-body problem, Journal of Physics: Condensed Matter **27**, 393001 (2015).

[36] K. Burke and J. Kozlowski, Lies my teacher told me about density functional theory: Seeing through them with the hubbard dimer, in *Simulating Correlations with Computers*, edited by E. Pavarini and E. Koch (Forschungszentrum Jülich GmbH Institute for Advanced Simulation, 2021) pp. 65–96.

[37] J. P. Perdew and M. Levy, Physical Content of the Exact Kohn-Sham Orbital Energies: Band Gaps and Derivative Discontinuities, Phys. Rev. Lett. **51**, 1884 (1983).

[38] L. J. Sham and M. Schlüter, Density-functional theory of the energy gap, Phys. Rev. Lett. **51**, 1888 (1983).

[39] C.-J. Huang and C. J. Umrigar, Local correlation energies of two-electron atoms and model systems, Phys. Rev. A **56**, 290 (1997).

[40] O. Gunnarsson and B. I. Lundqvist, Exchange and correlation in atoms, molecules, and solids by the spin-density-functional formalism, Phys. Rev. B **13**, 4274 (1976).

[41] O. Gunnarsson and R. O. Jones, Density functional calculations for atoms, molecules and clusters, Physica Scripta **21**, 394 (1980).

[42] O. Gunnarsson, M. Jonson, and B. Lundqvist, Exchange and correlation in inhomogeneous electron systems, Solid State Communications **24**, 765 (1977).

[43] K. Burke, J. P. Perdew, and Y. Wang, Derivation of a generalized gradient approximation: The pw91 density functional, in *Electronic Density Functional Theory: Recent Progress and New Directions*, edited by J. F. Dobson, G. Vignale, and M. P. Das (Springer US, Boston, MA, 1998) pp. 81–111.

[44] P. Romaniello, S. Guyot, and L. Reining, The self-energy beyond gw: Local and nonlocal vertex corrections, The Journal of Chemical Physics **131**, 154111 (2009), https://doi.org/10.1063/1.3249965.

[45] F. Aryasetiawan, Self-energy of ferromagnetic nickel in the gw approximation, Phys. Rev. B **46**, 13051 (1992).

[46] F. Aryasetiawan, L. Hedin, and K. Karlsson, Multiple plasmon satellites in na and al spectral functions from ab initio cumulant expansion, Phys. Rev. Lett. **77**, 2268 (1996).

[47] M. Guzzo, G. Lani, F. Sottile, P. Romaniello, M. Gatti, J. J. Kas, J. J. Rehr, M. G. Silly, F. Sirotti, and L. Reining, Valence electron photoemission spectrum of semiconductors: Ab initio description of multiple satellites, Phys. Rev. Lett. **107**, 166401 (2011).

[48] J. Kuneš, I. Leonov, P. Augustinský, V. Křápek, M. Kollar, and D. Vollhardt, LDA+DMFT approach to ordering phenomena and the structural stability of correlated materials, The European Physical Journal Special Topics **226**, 2641 (2017).

[49] X.-J. Zhang, E. Koch, and E. Pavarini, Origin of orbital ordering in $YTiO_3$ and $LaTiO_3$, Phys. Rev. B **102**, 035113 (2020).

[50] R. M. Martin, L. Reining, and D. M. Ceperley, *Interacting Electrons: Theory and Computational Approaches* (Cambridge University Press, 2016).

[51] A. Stan, N. E. Dahlen, and R. van Leeuwen, Levels of self-consistency in the GW approximation, The Journal of Chemical Physics **130**, 10.1063/1.3089567 (2009), 114105, https://pubs.aip.org/aip/jcp/article-pdf/doi/10.1063/1.3089567/15424617/114105_1_online.pdf.

[52] A. El-Sahili, F. Sottile, and L. Reining, Total energy beyond gw: Exact results and guidelines for approximations, Journal of Chemical Theory and Computation **0**, null (0), pMID: 38324673, https://doi.org/10.1021/acs.jctc.3c01200.